Running title: Complete life cycle of the bioluminescent California Sea Firefly

Laboratory culture of the California Sea Firefly *Vargula tsujii* (Ostracoda: Cypridinidae): Developing a model system for the evolution of marine bioluminescence

Jessica A. Goodheart[1], Geetanjali Minsky[1], Mira N. Brynjegard-Bialik[1], Michael S. Drummond[1], J. David Munoz[2], Timothy R. Fallon[3,4], Darrin T. Schultz[5,6], Jing-Ke Weng[3,4], Elizabeth Torres[2] & Todd H. Oakley*[1]

[1] Department of Ecology, Evolution, and Marine Biology, University of California, Santa Barbara, Santa Barbara, CA 93106

[2] Department of Biological Sciences, California State University, Los Angeles, CA 90032-8201, USA

[3] Whitehead Institute for Biomedical Research, Cambridge, MA, 02142, USA

[4] Department of Biology, Massachusetts Institute of Technology, Cambridge, MA 02142, USA

[5] Monterey Bay Aquarium Research Institute, Moss Landing, CA 95060, USA

[6] Department of Biomolecular Engineering and Bioinformatics, University of California, Santa Cruz, Santa Cruz, CA 96060, USA

*Corresponding author: oakley@lifesci.ucsb.edu

Abstract

Bioluminescence, or the production of light by living organisms via chemical reaction, is widespread across Metazoa. Culturing bioluminescent organisms from diverse taxonomic groups is important for determining the biosynthetic pathways of bioluminescent substrates, which may lead to new tools for biotechnology and biomedicine. Although some previously cultured luminescent groups represent independent origins of bioluminescence, cnidarians, ctenophores, and brittle stars use luminescent substrates (luciferins) obtained from their diets, and therefore are not informative for determination of the biosynthethic pathways of the luciferins. Terrestrial fireflies do synthesize their own luciferin, but the biosynthetic pathway for firefly luciferin remains unclear. An additional independent origin of endogenous bioluminescence is found within ostracods from the family Cypridinidae, which use their luminescence for defense and, in Caribbean species, for courtship displays. Here, we report the first complete life cycle of a luminous ostracod (*Vargula tsujii*, the California Sea Firefly) in the laboratory. We also describe the embryonic development of *Vargula tsujii* and discuss the size classes of instar development. We find embryogenesis in *V. tsujii* ranges between 25-38 days, and this species appears to have five instar stages, consistent with ontogeny in other cypridinid lineages. We estimate a complete life cycle at 3-4 months. We present the first complete mitochondrial genome for *Vargula tsujii*. Finally, we find no evidence of significant population genetic structure or cryptic species throughout the southern California range of *V. tsujii*. Bringing a luminous ostracod into laboratory culture sets the stage for many potential avenues of study, including the biosynthetic pathway of cypridinid luciferin and genomic manipulation of an autogenic bioluminescent system.

Keywords: ostracod, cypridinid, animal culture, cypridinid luciferin, embryogenesis, Crustacea

53 **Introduction**

54 The production of bioluminescence in animals is an important biological innovation that is
55 particularly prevalent in marine environments [1]. To produce light, animals combine an enzyme
56 (usually a luciferase or photoprotein) and a substrate (luciferin) with oxygen, and sometimes
57 additional components such as ATP or calcium [2–4]. Although the enzymes that produce light are
58 well-studied [5–13], and we know how the substrate is produced in bacteria [14] and fungi [15], we do
59 not yet know how luciferin is synthesized in any animal system. A comprehensive understanding
60 of this pathway could be transformative for optogenetics in transgenic organisms, where the
61 ability to produce bioluminescence in situ as a biosensor or light source would be invaluable.
62 Some laboratory-reared luminescent animals already exist (Table 1), but may not be suitable for
63 studying luciferin biosynthesis. In particular, ctenophores, cnidarians, and brittle stars use
64 coelenterazine obtained from their diet as a substrate [1]. Fireflies do use an endogenous luciferin
65 specific to Coleoptera (beetles) [16], but they often have longer life cycles than other taxa, slowing
66 research progress [17]. Although there are other independent origins of autogenic
67 bioluminescence, which we define as that produced via luciferase and luciferin that are
68 synthesized via the genome of the light producing animal, no laboratory cultures exist yet. This
69 makes additional studies focused on the comparative evolution of this ability extremely
70 challenging.

71

72 Ostracods from the family Cypridinidae independently evolved bioluminescence, and use a
73 luciferin that is endogenous to ostracods and chemically different from that of other
74 bioluminescent organisms [2,18,19]. Of the metazoan taxa already cultured, autogenic
75 luminescence is only known to occur within fireflies [20,21]. Due to the independent origin of
76 ostracod bioluminescence in the family Cypridinidae, and evidence for the autogenic nature of
77 the necessary luciferin and luciferase, ostracods represent a critical lineage for understanding
78 how bioluminescence evolved. Establishing laboratory cultures of luminescent ostracods within

79 Cypridinidae would pave the way for investigations into the biosynthetic pathway of luciferins in
80 Metazoa, as well as comparative studies of the biochemistry, physiology, genetics, and function
81 of endogenous bioluminescence.
82
83 Cypridinidae is estimated to include over 300 ostracod species [22], some of which use
84 bioluminescence for defense, while others possess the ability to create bioluminescent courtship
85 displays in addition to defensive secretions [23]. Lineages with sexually dimorphic bioluminescent
86 displays, such as those in Cypridinidae, have more species than their non-displaying sister
87 lineages, indicating that origins of bioluminescent courtship may increase diversification rates
88 (Ellis and Oakley 2016). As such, cypridinid ostracods represent an excellent system for
89 understanding how behavioral diversification can lead to increases in species accumulation.
90 Furthermore, cypridinid ostracods diversified while generating bioluminescence with a
91 consistent biochemical basis across the clade [24], meaning that they use the same luciferin and
92 homologous enzymes to make light. The conserved nature of the luminescent chemical reaction
93 provides a system within which bioluminescence can produce rapid changes in phenotypic
94 diversity by modifying amino acid sequences of the enzyme or how the enzyme is used [25].
95
96 Attempts to culture luminescent and non-luminescent species of Cypridinidae have led to
97 varying success, including *Skogsbergia lerneri* (non-luminous species with no mating in culture)
98 [26], *Photeros annecohenae* (luminous species without the complete life cycle in culture) [27], and
99 *Vargula hilgendorfii* (luminous species with no mating in culture) [28]. Researchers attempting to
100 culture *Vargula hilgendorfii* tried multiple alternative aquarium set-ups and tested sensitivity to
101 nutrients commonly measured in aquaria, but were still unable to induce mating in the lab [28]. An
102 unnamed species of luminescent ostracod is claimed to have been cultured at the CTAQUA
103 Foundation (Aquaculture and Technological Centre) in Spain for molecular gastronomy [29], but
104 no information on species, culture longevity, or whether mating occurred is available on this

enigmatic and uncertain culture. Other non-cypridinid ostracods have been reared in the laboratory as well, including the myodocopids *Euphilomedes carcharodonta* [30] and *Euphilomedes nipponica* [31] and the podocopid *Xestoleberis hanaii* (only record of copulation in the laboratory for any ostracod) [32].

In this paper, we present evidence that we are the first to rear a luminous ostracod (*Vargula tsujii*) through its complete life cycle in the laboratory. *Vargula tsujii* is the only bioluminescent cypridinid ostracod described from the Pacific coast of North America. Commonly found in southern California, the reported range of *V. tsujii* is from Baja California to Monterey Bay [33]. This species is primarily active in the kelp canopy at night [34]. Similarly to some other cypridinid ostracods, *Vargula tsujii* is a scavenger, and is presumed to feed on dead and decaying fish and invertebrates on the benthos since it can be collected via baited traps. However, some authors also observed *V. tsujii* attacking the soft tissues of live fishes caged nearshore [35]. *Vargula tsujii* is an important prey item of the plainfin midshipman fish (*Porichthys notatus*), as it is the source of luciferin for the bioluminescence seen in the fish [36].

In addition to evidence for the completion of the life cycle of *Vargula tsujii* in the laboratory, we provide a successful methodology for culturing individuals of *V. tsujii*, descriptions and analyses of embryogenesis and instar development, a reconstruction of its mitochondrial genome, and a brief description of the distribution of molecular diversity of *V. tsujii* across coastal southern California.

Methods

Specimen collection

We collected *Vargula tsujii* from three primary locations: (1) Fisherman's Cove near Two Harbors on Catalina Island, CA, USA (33°26'42.5"N 118°29'04.2"W) directly adjacent to the Wrigley Marine Science Center, (2) Cabrillo Marina, Los Angeles, CA, USA (33°43'13.5"N 118°16'47.4"W), and (3) Shelter Island public boat ramp, San Diego, CA, USA (32°42'56.3"N 117°13'22.9"W) (Figure 1; Table 2). We also provide locations in Figure 1 and Table 2 where we set traps but did not collect *V. tsujii*. The specimens used for culture and description of the life cycle of *V. tsujii* were exclusively from Fisherman's Cove, Catalina Island, and we collected additional specimens from the Cabrillo Marina and Shelter Island public boat ramp to discern the genetic diversity of *V. tsujii* and test for the presence of any cryptic species. For specimen collection we used Morin pipe traps: cylindrical polyvinyl chloride (PVC) tubes with mesh funnels to prevent the ostracods from escaping once they entered [37]. We baited traps with dead fish or fresh chicken liver (roughly 1-2 cm^3). We set traps in 1-10 meters of water at sunset and collected them 1.5 to 2 hours after last light to allow time for the ostracods to accumulate.

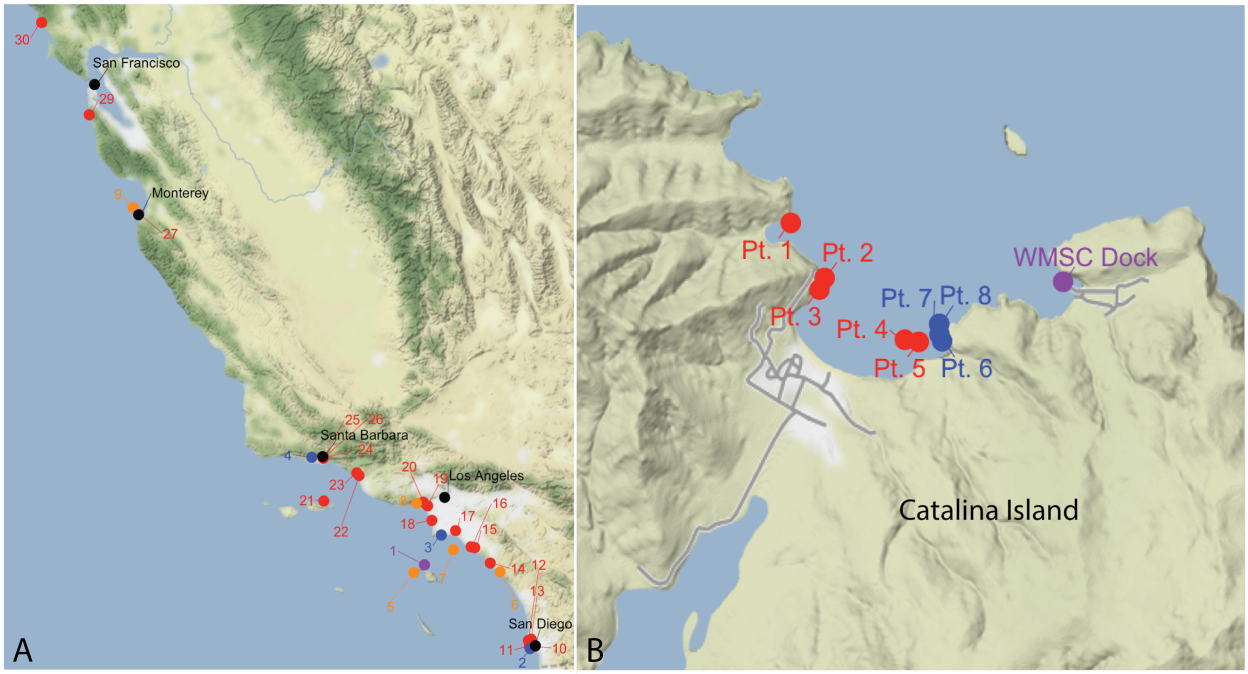

Figure 1. Map of localities where collections (and attempted collections of Vargula tsujii were made). Black points represent geographic annotations for reference, purple points refer to the location where ostracods were collected that were ultimately cultured, blue where animals were found or collected, orange where Kornicker originally collected animals, and red where no V. tsujii were found. (A) Map of the California (USA) coastline where V. tsujii collections were attempted; (B) Map of the region near Two Harbors (Santa Catalina Island, California, USA) where V. tsujii collections were attempted.

146 *Population genetic analyses*

147 We obtained *Vargula tsujii* sequence data for 16S rRNA (16S) and cytochrome oxidase 1 (COI)
148 from a previously published thesis [38]. We then aligned and visually inspected sequence
149 chromatograms with Sequencher version 3.1 (Gene Codes Corp) (Table S1). We constructed
150 haplotype networks for the two genes, COI (Number of individuals: Catalina, 18; San Diego, 11;
151 San Pedro, 12) and 16S (Number of individuals: Catalina, 19; San Diego, 20; San Pedro, 21)
152 (Figure 3) with the package pegas [39] in the R environment (version 3.4.2) [40]. To assess whether
153 sequences within populations cluster together, we analyzed each gene via Discriminant
154 Analysis of Principal Components (DAPC) using the adegenet package in R [41] and compared
155 models with one, two, and three clusters using the Bayesian Information Criterion (BIC) [42].

156

157 *Description of aquarium system and feeding*

158 We cultured *Vargula tsujii* at the University of California, Santa Barbara in aquariums designed
159 for water to flow through sand and out the bottom. This allowed continuous water flow to keep
160 water fresh, and not suck ostracods into a filter. Instead, ostracods remain in sand where they
161 spend the daylight hours. We kept animals under a 12:12 light cycle with an indirect blue LED
162 light.

163

164 We first modified a five gallon glass tank by drilling a hole in the bottom, which was then
165 covered with the bottom of an undergravel filter and a 3 cm layer of commercial aragonite sand
166 for aquariums. To maintain continuous water flow, we used plastic tubing (diameter = 1 cm)
167 connected directly to an overflowing reservoir tank, which created a siphon system for moving
168 water into the tank (Figure 2). The siphon provided continuous water flow when needed, and
169 prevented overflow of the aquarium. In addition, to prevent a complete drain of the water if the
170 siphon flow broke, which is common with larger siphons, we attached an outflow pipe to the
171 bottom of the aquarium that drained halfway up the side of the tank (Figure 2).

172

173 We also created a similar system for smaller experimental aquaria, though these appeared to
174 be less effective long-term, as we saw high mortality in non-systematic studies. For the small
175 aquaria ("condos"), we cut a large hole (~5 cm diameter) into the bottom of seven 500 mL
176 Nalgene™ Square PETG Media Bottles with Septum Closures (Figure 2F). We then modified a
177 100 μm cell strainer to fit in the bore of the media bottle in such a way that it would remain there
178 when the closure of the media bottle was screwed back on, allowing water but not sand to flow
179 through. We inverted the bottle and added a ~3 cm layer of sand to the bottom, above the cell
180 strainer, measured from the edge of the bottle cap. For these smaller aquaria, we used 5 mm
181 diameter tubing as siphons from the reservoir tank and for the outflow. Similar to the large tank,
182 the outflow tubes (placed in the septum closure) drained roughly halfway up the side of the
183 aquaria to prevent the water from draining completely.
184
185 Most recently, we created custom aquariums from acrylic (Fig. 2G), with similar dimensions to
186 the 5-gallon glass aquarium. We installed a bulkhead in the bottom and attached PVC tubing as
187 a drain, which we again raised to about half the height of the aquarium to prevent complete
188 drainage if inflow of water stops accidentally. We added a valve to control the rate of outflow
189 and instead of a siphon, we added a float switch to set inflow rate.
190
191

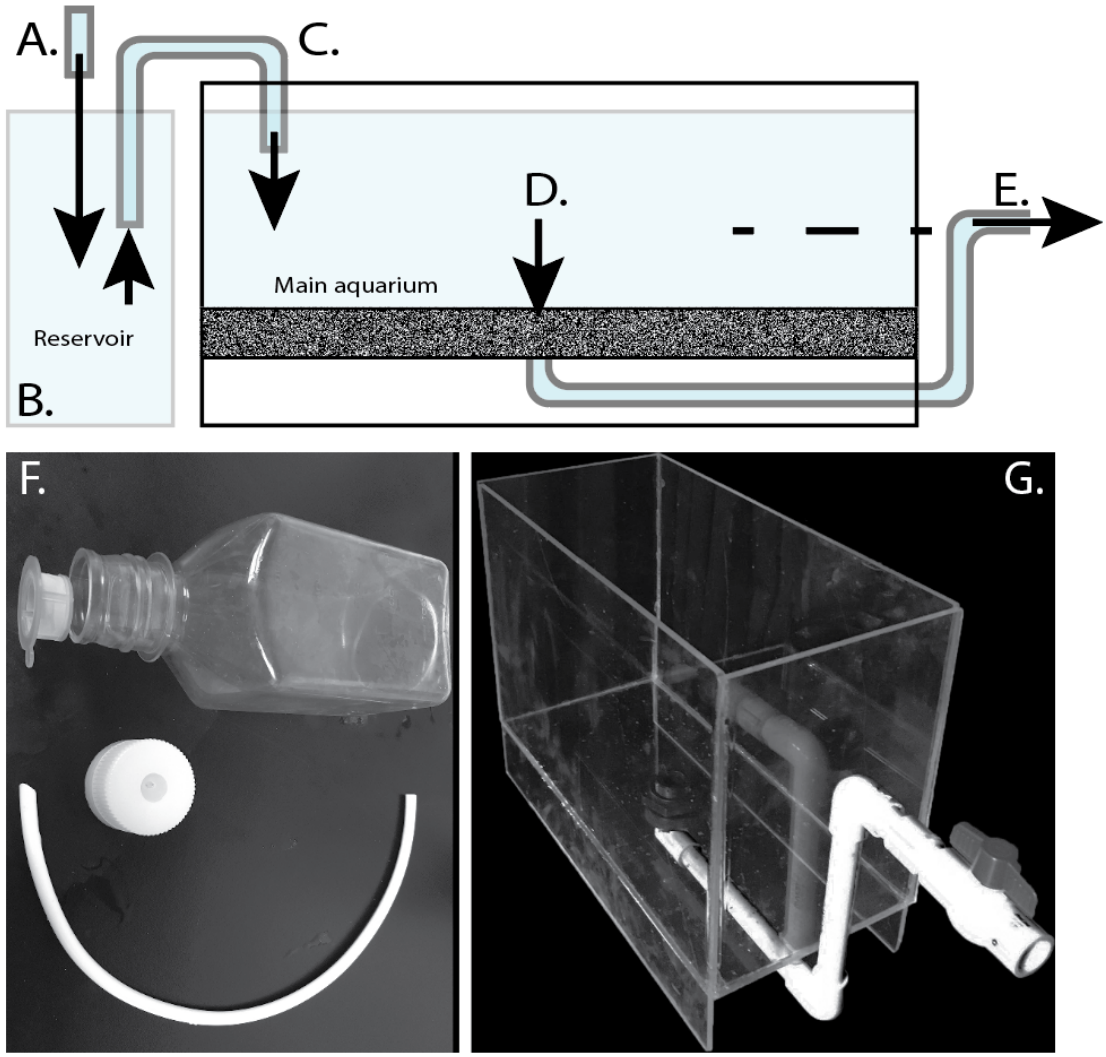

Figure 2. Diagrammatic representation of aquarium setup for sea fireflies. (A) Source water flows into (B) a reservoir tank, which overflows to keep the reservoir full and water level constant. (C) We use a siphon to carry water from a reservoir tank to main aquarium where ostracods live. Water level of the main tank drains through sand (stippled), through (E) an outflow that is raised to a level that would cause water to remain at the level of the dashed line, even if a siphon is interrupted to cause water to stop flowing into the main tank. (F) Plastic bottle and parts used to create small aquarium using the same logic as main aquarium. (G) Custom-built acrylic aquarium with drain in bottom and raised outflow with adjustable rate.

We initially offered the ostracods multiple diet choices, including: (1) imitation crab, which is primarily pollock, (2) carnivore fish pellets or fish flakes, (3) tilapia fillets, and (4) anchovies, which have each made for successful food sources in Caribbean ostracods (Todd Oakley, personal observation; [27,37]). Although the adults appeared moderately interested in these food sources in non-systematic trials, we found the juvenile ostracods did not eat them, but they did

202 actively feed on raw chicken liver, as do *Vargula hilgendorfii* individuals from Japan [43]. In
203 culture, we therefore provided pieces of chicken liver daily (~1 cm^3 per 200 animals). Due to the
204 nocturnal life history of *V. tsujii*, we fed them in the late afternoon or early evening (around the
205 beginning of the dark cycle), and removed the food from the aquarium in the morning (~3-5
206 hours into the light cycle) to reduce the chance of bacterial fouling.
207
208 *Rearing of embryos*
209 We tested two primary methods for rearing embryos. The first was less successful in terms of
210 longevity of both the mothers and embryos, but provided usable data on embryogenesis.
211 Regardless of rearing method, ostracods did not appear to eat while they were brooding.
212
213 For the first method, we kept females individually in circular wells in twelve-well dishes [27], with
214 approximately 1 mL of 17°C seawater. We recorded visual observations of the females and their
215 embryos and changed the water daily. The advantage of this method is ease of identification
216 and observation of individual ostracods, allowing us to track the growth of specific embryos over
217 a given period of time. However, all females which deposited embryos into the brooding
218 chamber died before their embryos were released from the marsupium, although the precise
219 cause of death is unknown. These embryos were then removed from the female marsupium by
220 dissection, kept in wells, and observed until the animals hatched through the chorion (see
221 Supplemental Video).
222
223 For the second method, we identified and removed brooding females from the aquarium and
224 placed them in 50 mL Falcon™ tubes (2 females per tube). Roughly 5 mL of sand was added to
225 the bottom of each tube to allow females to burrow. Falcon tubes were then placed in a large
226 seawater reservoir that ranged from 17-19°C. We changed the water in each tube daily, and

227 imaged brooding females every other day with a camera attached to a dissecting scope. We
228 used key diagnostic features such as number of embryos and female size to distinguish
229 individual females from one another. Of the thirteen individuals kept in Falcon™ tubes, only one
230 died prior to embryo release from the marsupium.
231
232 *Animal measurements and determination of instar size classes*
233 We imaged ostracods across all life stages using a standard dissecting microscope and an
234 Olympus brand camera, and measured the carapace length, carapace height, eye width, and
235 keel width with the software Fiji (Sample size = 626 individuals; Table S3)[44]. These parameters
236 are useful in the determination of the instar stages in other bioluminescent ostracods [27]. A
237 subset of these individuals (9 males, 11 females) were dissected to confirm sex. We partitioned
238 the data into clusters using the KMeans clustering algorithm implemented in scikit-learn [45] in
239 Python 2.7 [46]. KMeans fits the data into k clusters, specified in the arguments, sorting each data
240 point into the cluster which has the minimum euclidean distance to the centroid of the cluster.
241 The value for k was originally specified as eight based on the five known stages of instar
242 development for related species of ostracods plus the embryonic stage and adult males and
243 females. However, a k-value of eight clusters resulted in a split of the inferred adult female
244 cluster into two clusters rather than the discrimination of adult males from inferred A-I instars. To
245 avoid this apparent over-clustering, we ran our final analysis with a k-value of seven, which
246 retained all inferred adult females in a single cluster but was unable to distinguish an adult male
247 cluster from the inferred A-I instars. We assigned development stages to each cluster based on
248 the relationship by comparison to the closely related *Photeros annecohenae*, which grew in 12-
249 well dishes to allow more precise documentation of instars [27].
250
251 *Whole genome sequencing*

252 We froze four adult female *Vargula tsujii*, collected from the WMSC Dock on 2017-09-01 in
253 liquid nitrogen and shipped the specimens on dry-ice to the Hudson Alpha Institute for
254 Biotechnology Genomic Services Lab (HAIB-GSL) for genomic DNA extraction and Chromium
255 v2 Illumina sequencing library preparation. HAIB-GSL extracted the DNA using the Qiagen
256 MagAttract Kit, yielding 141 ng, 99 ng ,153 ng , and 96 ng of extracted DNA respectively. This
257 quantity of DNA was not sufficient for a size distribution analysis via agarose pulse field gel
258 analysis, therefore we decided to proceed with Chromium v2 library prep with the 153 ng
259 sample (sample # 5047), without confirmation of a suitable high-molecular weight DNA size
260 distribution. We sequenced this library on three lanes of a HiSeqX instrument using a 151x151
261 paired-end sequencing mode, resulting in a total of 910,926,987 paired reads (260.6 Gbp). We
262 attempted whole genome assembly of the resulting sequencing data with the Supernova v2.0.0
263 genome assembly software [47]. We then used the Agilent Femto Pulse High Molecular Weight
264 DNA capillary electrophoresis instrument at the MIT BioMicro Center to perform a post
265 sequencing analysis of the size distribution of the DNA used for Chromium library preparation.
266
267 *Mitochondrial genome assembly*
268 To achieve a full length mitochondrial genome (mtDNA) assembly of *V. tsujii*, we partitioned and
269 assembled sequences separately from the nuclear genome. We mapped Illumina reads from
270 our Chromium libraries (Table S3) to the known mtDNA of the closest available relative, *Vargula*
271 *hilgendorfii* (NC_005306.1) [48] using bowtie2 (v2.3.3.1)[49] (parameters: --very-sensitive-local). We
272 then extracted read pairs with at least one read mapped from the resulting BAM file with
273 samtools (parameters: view -G 12), then name-sorted, extracted in FASTQ format (parameters:
274 samtools fastq) and input the reads into SPAdes (v3.11.1)[50] for assembly (parameters: --only-
275 assembler -k55,127). Inspection of the resulting assembly graph using Bandage (v.0.8.1)[51],
276 combined with a heuristic manual deletion of low coverage nodes (deletion of nodes with
277 coverage <200x, mean coverage ~250x) gave rise to two loops with sequence similarity to the

278 *V. hilgendorfii* mtDNA that both circularized through a single path (Supplementary Figure 1.8.1).
279 We then manually inspected this graph via a blastn(2.7.1+)[52] aligned against the *V. hilgendorfii*
280 mtDNA through SequenceServer (v1.0.11)[53] and visualized with the Integrated Genomics
281 Viewer (v2.4.5)[54]. We noted that the single circularizing path was homologous to the two
282 duplicated control regions reported in the *V. hilgendorfii* mtDNA [48]. We surmised that this
283 assembly graph structure indicated the *V. tsujii* mtDNA had the same global structure as the *V.*
284 *hilgendorfii* mtDNA, and so used the Bandage "specify exact path" tool to traverse the SPAdes
285 assembly graph and generate a FASTA file representing the circularized *V. tsujii* mtDNA with
286 the putative duplicated control regions (Figure S1). To avoid splitting sequence features across
287 the mtDNA circular sequence break, we circularly rotated this full assembly with the seqkit
288 (v0.7.2)[55] "restart" command, to set the first nucleotide of the FASTA file at the start codon of
289 ND2. We then confirmed 100% of the nucleotides via bowtie2 re-mapping of reads and
290 polishing with Pilon (v1.21)[56] (parameters: --fix all). We annotated the final assembly of the
291 mitochondrial genome using the MITOS2 web server [57] with the invertebrate mitochondrial
292 genetic code (translation table 5). We manually removed low confidence and duplicate gene
293 predictions from the MITOS2 annotation.
294
295 **Results**
296 *Population genetics analyses*
297 Our COI haplotype network revealed minimal structure among *V. tsujii* populations in southern
298 California (Figure 3A). Haplotypes from San Pedro and Catalina Island overlap or diverge by
299 only one to three mutations. Haplotypes from San Diego individuals, although still very similar to
300 haplotypes from Catalina Island and San Pedro, differ by at least eight mutations and show no
301 overlap with haplotypes from other populations of *V. tsujii*. However, the haplotype network for
302 16S indicates that sequences from San Diego individuals are identical to some individuals from
303 the other two populations. Furthermore, although the model with three clusters was favored in

304 the DAPC analysis for each gene (Supplementary Materials S2 and S3), membership in five of
305 the six clusters includes individuals from different populations (Supplementary Materials S4 and
306 S5). Therefore our analyses do not support three genetically distinct populations as defined by
307 location.
308
309

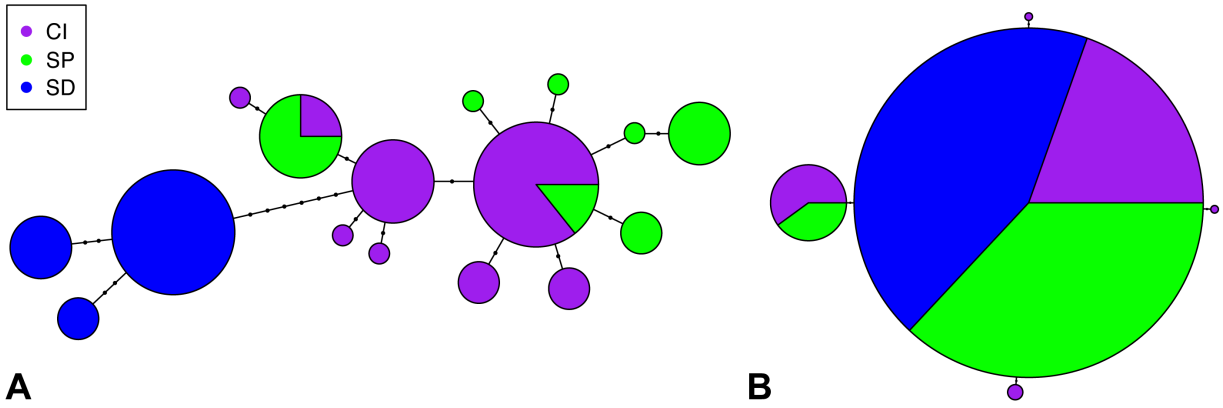

310

311 **Figure 3.** Haplotype networks for (A) COI sequences, and (B) 16S sequences of Vargula tsujii animals from three localities sampled. Abbreviations: CI, Catalina Island; SD, San Diego; SP, San Pedro.
312

313 *Embryogenesis Description*

314 After fertilization and release into the marsupium, *V. tsujii* embryos resemble opaque, green,
315 ovoidal embryos (Figures 4 and 5). After five to eight days of growth, separation of the yolk
316 begins, which appears as a light green mass condenses within the embryo. Around ten to
317 eighteen days after deposition into the brooding chamber, two very small red lateral eyespots
318 are visible on each embryo and the separation of the yolk continues. Daily observations over the
319 next six days showed continual growth and darkening of the eyes. By day sixteen the yolk is
320 almost completely separated and has begun to form the gut of the ostracod. By days fifteen to
321 nineteen, the eyespots are mostly black and the light organ (a light brown/yellow mass) appears
322 anteroventral to the eyes of the embryo. Around twenty days after deposition, developing limbs
323 in the form of two rows of small brown masses are visible along the ventral side of the embryos.

At this point the gut has finished forming within the carapace and is visible as a yellow-white mass on the posterior end of each embryo. Limb formation continues over the next few days, and the eyes of each embryo become entirely black. Twenty-five to thirty-eight days following embryo deposition, embryogenesis is complete, and instars are released from the mother's marsupium.

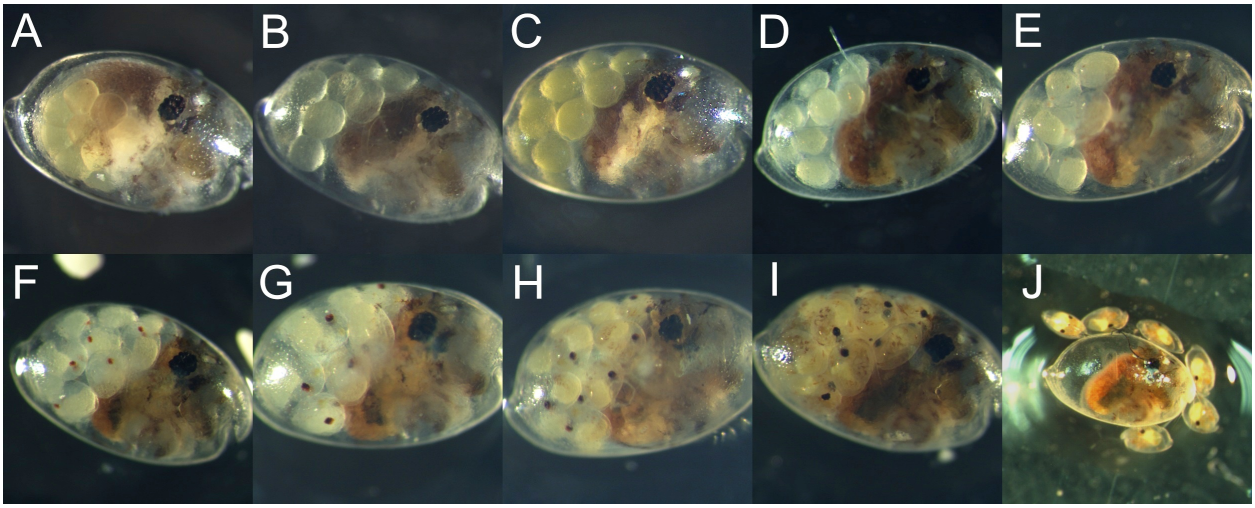

Figure 4. Embryogenesis within brooding females of V. tsujii post release into the marsupium. (A) Day 0, (B) Day 1-4, (C) Day 5-7, (D) Day 8-9, (E) Day 10-13, (F) Day 14-17, (G) Day 18-19, (H) Day 20-21, (I) Day 22-23, (J) Day 25-39.

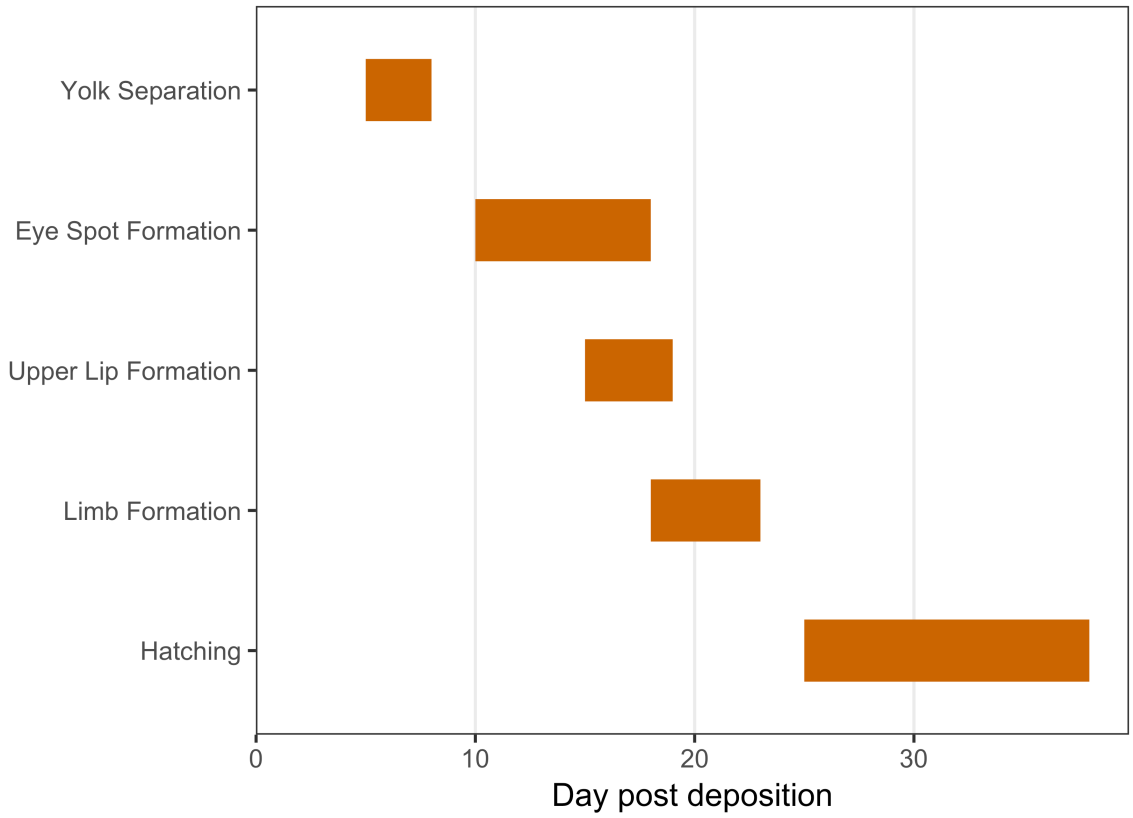

339

340 **Figure 5.** Summary of the timing of embryogenesis stages in V. tsujii. This represents the complete range of first appearance of each features across multiple broods, including: yolk separation (range = 5-8 days, N = 7); eye spot formation (range = 10-18 days, N = 12); upper lip formation (range = 15-19 days, N = 3); limb formation

341 (range = 18-23 days, N = 11); hatching (range = 25-38 days, N = 11).

342 *Instar development*

343 Vargula tsujii has five inferred juvenile instar stages (A-I, A-II, A-III, A-IV, A-V) and an adult

344 stage, most of which have a conserved size range (Figure 6A; Table 3). Laboratory

345 measurements of specimens of unknown sex were compared with the measurements of sexed

346 individuals (9 males, 11 females) to confirm interpretation of the instar stage of size classes

347 (Figure 6C-D). Due to large amounts of overlap of A-1 females with adult and A-I males, these

348 three groups are currently indistinguishable in our data set. Sexual dimorphism becomes

349 apparent in adulthood, with adult females clearly larger than adult males. However, compared to

350 many other cypridinid ostracods, this dimorphism can be difficult to assess visually without a

351 side-by-side comparison.

352 *Evidence for complete life cycle in the lab*

To assess whether a complete life cycle was obtained in the laboratory, we began with only brooding females in a small experimental aquarium. Those brooding females, although not tracked individually, released a number of juveniles, which we measured intermittently over time (Figure 6B). In this aquarium we found juveniles, and eventually adults, that fell across the full size range of wild-caught ostracods. After all of the broods hatched, we removed all adult females from the experimental aquarium to assess whether the ostracods would mature and mate in the laboratory. Following removal of the original adult females, we found adult brooding females that grew up in experimental aquarium that themselves gave birth to the next generation in 3-4 months time.

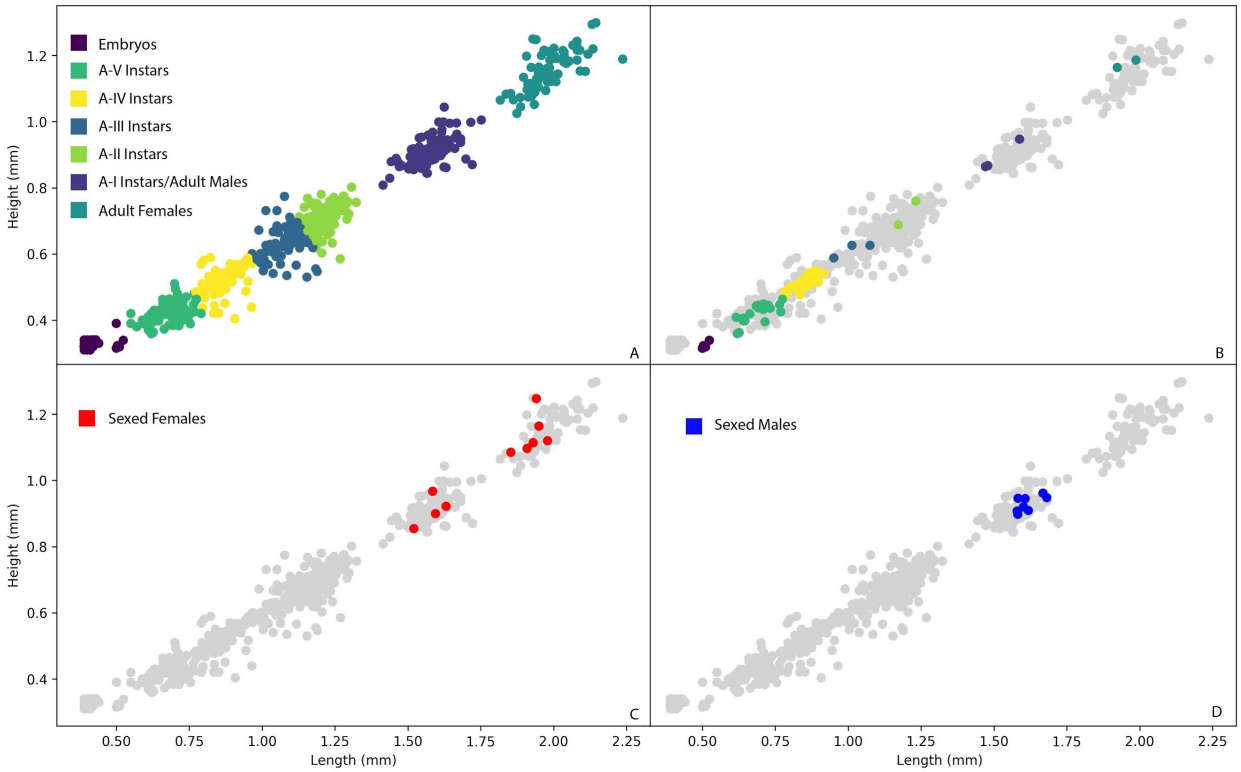

Figure 6. (A) K-means clusters of Vargula tsujii developmental stages based on carapace height and width. Instar stages were assigned to each cluster via comparison to P. annecohenae and additional analysis of male and female size dimorphism. (B) Points representing laboratory cultured animals overlayed on wild caught and unknown data. Different colors represent different clusters in the k-means analysis, and are labeled with their inferred instar/adult stages. (C) Shows wild-caught animals dissected and identified as female in relation to the k-means clusters, and (D) shows wild-caught animals dissected and identified as male in relation to the k-means clusters.

368 *Nuclear and mitochondrial genome assemblies*

369 Our final *Vargula tsujii* nuclear genome assembly is highly fragmented, with an indication of high
370 levels of heterozygosity between haplotypes (~5%) and a high proportion of simple sequence
371 repeats. Our post-sequencing analysis indicated the mode of the DNA size distribution for the
372 four extracted DNA samples were 1244 bp, 3820 bp, 1285 bp (sample #5047), and 1279 bp,
373 respectively, with a tail of ~20-40 kbp in each sample.

374

375 The final *V. tsujii* mtDNA (15,729 bp) (Figure 7) aligned to the previously published *V.*
376 *hilgendorfii* mtDNA [48] with 98% coverage and 78.5% nucleotide identity, and is available on
377 NCBI GenBank (MG767172). The *V. tsujii* mtDNA contains 22 tRNA genes, 13 protein coding
378 genes, and 2 duplicated control regions in an identical positioning and orientation to the *V.*
379 *hilgendorfii* mtDNA. There is one polymorphic base in the final mitogenome assembly coding for
380 a synonymous wobble mutation in the COII gene (COII:L76).

381

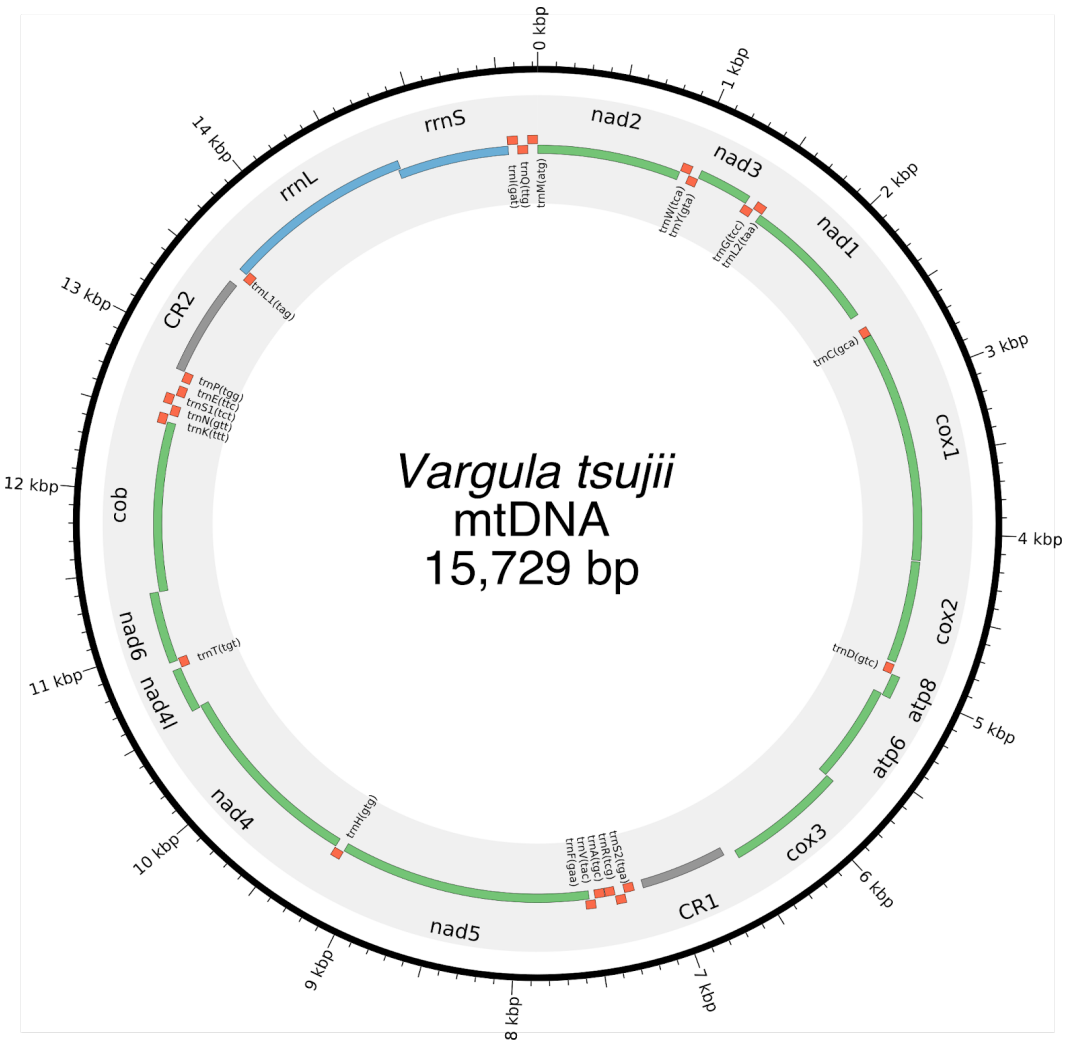

Figure 7. Mitochondrial genome of V. tsujii. Note the duplicated control regions, CR1 and CR2 (in gray). Figure produced with Circos [80].

Discussion

Based on measurement data on the first and second generations of ostracods reared in the lab (Figure 5), and the presence of brooding female ostracods in our experimental aquarium where adult females had previously been removed, we can infer that we were successful in rearing *Vargula tsujii* through its complete life cycle in the lab. This is a first for any bioluminescent ostracod, as rearing in the lab has remained a significant hurdle for laboratory studies in these animals [26–28]. Our current population was cultured from animals collected near Wrigley Marine Science Center on Santa Catalina Island, which appears to contain much of the genetic

393 diversity sampled across much of the known the range of *V. tsujii* (Figure 3). Our population
394 genetics analyses support the hypothesis that populations of *Vargula tsujii* experience some
395 gene flow across the localities sampled, including Catalina Island. These results are consistent
396 with the hypothesis that *V. tsujii* represents a single, connected species. As such, we assume
397 our culture of ostracods from Santa Catalina Island, and inferences made from it, may be
398 representative of the genetic diversity of populations of *V. tsujii* across southern California
399 coastal systems. However, we cannot discount the possibility that there might be some variation
400 in development times and instar sizes across the range of this species. Also of note is that this
401 species is not easily collected throughout the reported range, and northern populations, if they
402 exist, may be divergent from southern California populations.
403
404 *Attempted whole genome reconstruction*
405 The 1C genome size of *Vargula tsujii* was previously reported to be 4.46 ± 0.08 pg (Female,
406 n=3), and 4.05 pg (Male, n=1) [58], corresponding to a 1C genome size of 4.36 Gbp and 3.96 Gbp
407 respectively and suggesting XO sex determination. Our reconstruction of the *Vargula tsujii*
408 nuclear genome assembly is highly fragmented, with an indication of high levels of
409 heterozygosity between haplotypes (~5%) and a high proportion of simple sequence repeats.
410 We speculate that our poor nuclear genome assembly results are likely due to the small size
411 distribution of the input DNA, as larger fragment sizes are especially critical for the
412 reconstruction of large genomes such as *V. tsujii*. Further protocol development is needed to
413 extract suitable High Molecular Weight DNA, which could allow long-read sequencing that would
414 improve assembly.
415
416 *The life cycle of* Vargula tsujii
417 The embryogenesis of *Vargula tsujii* is similar to closely related species, and the 24-day
418 average brooding duration falls within the range for other cypridinid ostracods (10-30 days) [59].

419 The primary stages of *V. tsujii* embryonic development are yolk separation, formation of eye
420 spots, development of the upper lip, development of limbs, and emergence from the chorion and
421 marsupium (Figure 5). In general, the embryonic development of *Vargula tsujii* is longer than
422 that of other luminescent ostracods whose development has been described (Table 4).
423 However, early embryonic development in *V. tsujii* is faster than in *P. annecohenae*. In *P.*
424 *anncohenae,* yolk separation begins on day 9 and eye development begins on days 14-15 [27],
425 while those stages begin at 5-7 and 10-13 days, respectively, in *V. tsujii*. Additionally, the order
426 of development in *V. tsujii* appears to differ from that of *Vargula hilgendorfii,* which starts to
427 develop limbs on days 4-5, before eye and upper lip development [27,60]. By contrast, *V. tsujii* limbs
428 do not appear until after eye-spot and upper lip formation. The reasons for this difference are
429 unclear.
430
431 Juvenile development of *Vargula tsujii* is also quite similar overall to that of *Photeros*
432 *annecohenae*, the only other bioluminescent cypridinid ostracod for which instar developmental
433 data is available [27]. We inferred five distinct instar stages (A-V through A-I), and A-I instars
434 develop into size dimorphic adult males and females (Table 3). Average measurements of size,
435 including carapace length and height, as well as eye width, were comparable between
436 respective instar stages in *V. tsujii* and *P. annecohenae*. However, in *V. tsujii* average eye width
437 remains within the range of 0.060 mm to 0.0684 mm from the embryonic stage until the second
438 instar, and makes a large jump by about two fold in the third instar (0.121 ± 0.0208 mm), as
439 compared to a gradual increase in eye size in *P. annecohenae*. In our k-means clustering
440 analysis, the second-to-largest cluster of *V. tsujii* appears to contain adult males as well as A-I
441 males and females. This finding differs from that in *P. annecohenae*, where adult males were
442 found to cluster separately from A-I males and females and adult females based on size and
443 shape, and A-I males and females could be distinguished by certain shape parameters [27]. We
444 hypothesize that this apparent reduction of sexual dimorphism observed in the later stages of

445 development may occur because *V. tsujii* may have lost the ability to use luminescence for
446 courtship, so selection acting on differences in male and female shape may have been reduced.
447
448 *Benefits of completing the life cycle*
449 Cypridinid ostracods represent an independent origin of endogenous autogenic
450 bioluminescence. This group is a natural comparison to other, well-studied bioluminescent
451 courtship systems, such as that of fireflies [61]. Other possible laboratory models for
452 bioluminescence, such as brittle stars [62] and cnidarians [63] are useful for some research tasks,
453 such as studies of luciferins obtained from the diet (e.g., coelenterazine). Others might be easier
454 to rear in the laboratory, such as the self-fertilizing brittle star *Amphiolus squamata* [64]. However,
455 ostracods produce their own luciferase and luciferin, unlike brittle stars and cnidarians.
456 Ostracods also have relatively fast generation times (on the order of months), which can be
457 modified somewhat by adjusting the temperature of the water, as is common among ostracods
458 [26–28,65,66]. In comparison, fireflies are usually on a six-month to one-year life cycle that is difficult to
459 alter [67–69], and some brittle stars appear to spawn only seasonally [70,71]. Furthermore, culture of an
460 organism (*Vargula tsujii*) from a clade with an independent origin of autogenic bioluminescence
461 allows for comparative studies between luminescence in ostracods and the autogenic
462 bioluminescence found in fireflies [16] or other organisms, which would not otherwise be possible.
463
464 Ostracods will be incredibly useful for studying the physiology and biochemistry of
465 bioluminescence [2], as both diversification and behavioral changes in cypridinids related to
466 luminescence have occurred using the same luciferin and homologous luciferases [24].
467 Furthermore, ostracod courtship signals are bright and easily simulated in a laboratory setting,
468 allowing for assessments of male and female behavior in response to changes in signal
469 parameters, such as intensity, color, and pulse duration (e.g., [72]). These tools provide
470 researchers with an excellent system for asking important questions related to selection on

genes important for rapid diversification [73], including those related to behavior [74], sexual selection [75], and the role of the biochemical properties of bioluminescence [25].

Importantly, the biosynthetic pathway for luciferin production is currently unknown for any animal system. One major obstacle to describing this pathway has been building laboratory cultures for animal species that produce luciferin themselves and also have a relative fast generation time. Solving this bottleneck to accessing specimens for bioluminescent ostracods has set the stage for investigations into the biosynthetic pathway of cypridinid luciferin and its possible use in biomedical tools such as optogenetics [76]. Finally, this is an excellent system with which to consider developing genome editing techniques (e.g., CRISPR/Cas9) [77] to test candidate genes for luciferin biosynthesis, and to assess how genetic variants in critical genes might affect production or perception of bioluminescent signals.

Acknowledgements

We thank the USC *Wrigley Institute* for *Environmental Studies* for transportation and use of the facilities at the Wrigley Marine Science Center on Catalina Island, CA. JDM worked on the project at Wrigley during the Catalina Marine Biology Semester hosted by California State University and with support from the NSF (Award DEB·1457462 to ET). Population genetic work was supported by a mini-grant from Cal State LA to ET; sequence data were obtained from the Masters thesis of KH Lee; DM Jacinto and E Stiner helped with collections throughout California; RM Serrano helped with measurements of some specimens; N Hensley contributed data on collecting locations. Genomic sequencing was supported by the Beckman Young Investigator Award to JKW from the Arnold and Mabel Beckman Foundation and by a UCSB Faculty Seed Grant to THO.

497 **Author contributions**

498 JAG, ET, JKW, and THO conceived of and designed the study; JAG, GM, MNB, MSD, JDM,
499 TRF, and DTS contributed to the acquisition and analysis of the data in this study; all authors
500 participated in the interpretation of data, helped draft or substantially revise the manuscript, and
501 gave final approval for publication.

502

503 **Competing interests**

504 The authors declare no competing interests.

505

506 **Data availability**

507 Sequence data for COI and 16S are available in GenBank (Table S1) and our whole genome
508 Chromium reads are available in the Sequence Read Archive (SRR9308458). Scripts and data
509 for the population genetics and k-means clustering analyses are provided on Github
510 (https://github.com/goodgodric28/vargula_tsujii_culture). An additional video which shows
511 *Vargula tsujii* hatching from the chorion and outside the mother is provided on Youtube
512 (https://youtu.be/8o5CqHTcTjI).

513

514 **References**

515 1. Haddock, S. H. D., Moline, M. A. & Case, J. F. Bioluminescence in the sea. *Ann. Rev. Mar.*
516 *Sci.* **2**, 443–493 (2010).
517 2. Hastings, J. W. Biological diversity, chemical mechanisms, and the evolutionary origins of
518 bioluminescent systems. *J. Mol. Evol.* **19**, 309–321 (1983).
519 3. Shimomura, O., Johnson, F. H. & Saiga, Y. Extraction, purification and properties of
520 aequorin, a bioluminescent protein from the luminous hydromedusan, *Aequorea*. *J. Cell.*
521 *Comp. Physiol.* **59**, 223–239 (1962).

522 4. Tsuji, F. I. ATP-dependent bioluminescence in the firefly squid, *Watasenia scintillans*. *Proc.*
523 *Natl. Acad. Sci. U. S. A.* **82**, 4629–4632 (1985).
524 5. Cormier, M. J., Wampler, J. E., Hori, K. & Lee, J. W. Bioluminescence of *Renilla reniformis*.
525 IX. Structured bioluminescence. Two emitters during both the in vitro and the in vivo
526 bioluminescence of the sea pansy, *Renilla*. *Biochemistry* **10**, 2903–2909 (1971).
527 6. Dunlap, P. Biochemistry and Genetics of Bacterial Bioluminescence in *Advances in*
528 *Biochemical Engineering/Biotechnology* 37–64 (2014).
529 7. Fallon, T. R. *et al.* Firefly genomes illuminate parallel origins of bioluminescence in beetles.
530 *Elife* **7**, (2018).
531 8. Sweeney, B. The Bioluminescence of Dinoflagellates in *Biochemistry and Physiology of*
532 *Protozoa* 287–306 (1979).
533 9. Kobayashi, K. *et al.* Purification and properties of the luciferase from the marine ostracod
534 *Vargula hilgendorfii* in *Bioluminescence and Chemiluminescence* (2001).
535 doi:10.1142/9789812811158_0022
536 10. Hastings, J. W., Vergin, M. & Desa, R. Scintillons: The Biochemistry of Dinoflagellate
537 Bioluminescence in *Bioluminescence in Progress* 301–330 (Princeton University Press,
538 1967).
539 11. Nakatsu, T. *et al.* Structural basis for the spectral difference in luciferase bioluminescence.
540 *Nature* **440**, 372–376 (2006).
541 12. Marques, S. M. & Esteves da Silva, J. C. G. Firefly bioluminescence: a mechanistic
542 approach of luciferase catalyzed reactions. *IUBMB Life* **61**, 6–17 (2009).
543 13. Verhaegent, M. & Christopoulos, T. K. Recombinant *Gaussia* luciferase. Overexpression,
544 purification, and analytical application of a bioluminescent reporter for DNA hybridization.
545 *Anal. Chem.* **74**, 4378–4385 (2002).
546 14. Dunlap, P. V. & Urbanczyk, H. Luminous Bacteria. *The Prokaryotes* 495–528 (2013).
547 doi:10.1007/978-3-642-30141-4_75

548 15. Kotlobay, A. A. *et al.* Genetically encodable bioluminescent system from fungi. *Proc. Natl.*
549 *Acad. Sci. U. S. A.* **115**, 12728–12732 (2018).
550 16. Kanie, S., Nakai, R., Ojika, M. & Oba, Y. 2-S-cysteinylhydroquinone is an intermediate for
551 the firefly luciferin biosynthesis that occurs in the pupal stage of the Japanese firefly, *Luciola*
552 *lateralis*. *Bioorg. Chem.* **80**, 223–229 (2018).
553 17. McLean, M., Buck, J. & Hanson, F. E. Culture and larval behavior of photurid fireflies. *Am.*
554 *Midl. Nat.* **87**, 133 (1972).
555 18. Thompson, E. M., Nagata, S. & Tsuji, F. I. Cloning and expression of cDNA for the luciferase
556 from the marine ostracod *Vargula hilgendorfii*. *Proc. Natl. Acad. Sci. U. S. A.* **86**, 6567–6571
557 (1989).
558 19. Oba, Y., Kato, S.-I., Ojika, M. & Inouye, S. Biosynthesis of luciferin in the sea firefly,
559 *Cypridina hilgendorfii*: l-tryptophan is a component in *Cypridina* luciferin. *Tetrahedron Lett.*
560 **43**, 2389–2392 (2002).
561 20. de Wet, J. R., Wood, K. V., Helinski, D. R. & DeLuca, M. Cloning of firefly luciferase cDNA
562 and the expression of active luciferase in *Escherichia coli*. *Proc. Natl. Acad. Sci. U. S. A.* **82**,
563 7870–7873 (1985).
564 21. Seliger, H. H., McElroy, W. D., White, E. H. & Field, G. F. Stereo-specificity and firefly
565 bioluminescence, a comparison of natural and synthetic luciferins. *Proc. Natl. Acad. Sci. U.*
566 *S. A.* **47**, 1129–1134 (1961).
567 22. Morin, J. G. Luminaries of the reef: The history of luminescent ostracods and their courtship
568 displays in the Caribbean. *Journal of Crustacean Biology* **39**, 227–243 (2019).
569 23. Cohen, A. C. & Morin, J. G. Sexual morphology, reproduction and the evolution of
570 bioluminescence in Ostracoda. *Paleontological Society Papers* **9**, 37 (2003).
571 24. Morin, J. G. Based on a review of the data, use of the term ‘cypridinid’ solves the
572 *Cypridina*/*Vargula* dilemma for naming the constituents of the luminescent system of
573 ostracods in the family cypridinidae. *Luminescence* **26**, (2011).

25. Hensley, N. M. *et al.* Phenotypic evolution shaped by current enzyme function in the bioluminescent courtship signals of sea fireflies. *Proc. R. Soc. B* **286**, 20182621 (2019).

26. Cohen, A. C. Rearing and postembryonic development of the myodocopid ostracode *Skogsbergia lerneri* from coral reefs of Belize and the Bahamas. *J. Crustacean Biol.* **3**, 235–256 (1983).

27. Gerrish, G. A. & Morin, J. G. Life Cycle of a Bioluminescent Marine Ostracode, *Vargula annecohenae* (Myodocopida: Cypridinidae). *J. Crustacean Biol.* **28**, 669–674 (2008).

28. Wakayama, K & Kanazawa, K. Elucidation of environmental tolerance of sea fireflies and research on construction of optimal rearing environment *Sci. J. Kangawa U.* **25**, 117-124 (2014).

29. Pérez-Lloréns, J. L. Cooking-Science-Communication (CSC): The ideal trident to enjoy the dining experience. *International Journal of Gastronomy and Food Science* **16**, 100134 (2019).

30. Koyama, K. H. & Rivera, A. S. Embryonic development of the myodocopid ostracod *Euphilomedes carcharodonta* Smith, 1952. *J. Crustacean Biol.* (2018). doi:10.1093/jcbiol/ruy088

31. Kawamata, K., Sato, M. & Abe, K. Complete life cycle of the ostracod *Euphilomedes nipponica* (Myodocopida, Philomedidae). *Plankton Benthos Res.* **13**, 83–89 (2018).

32. Ikeya, N. & Kato, M. The life history and culturing of *Xestoleberis hanaii* (Crustacea, Ostracoda) in *Evolutionary Biology and Ecology of Ostracoda* (eds. Horne, D. J. & Martens, K.) 149–159 (Springer Netherlands, 2000).

33. Korniker, L. S. & Baker, J. H. *Vargula tsujii*, a new species of luminescent ostracod from lower and southern California (Myodocopa: Cypridininae). *Proceedings of the Biological Society of Washington* **90**, 218–231 (1977).

34. Hammer, R. M. Day-night differences in the emergence of demersal zooplankton from a sand substrate in a kelp forest. *Mar. Biol.* **62**, 275–280 (1981).

600 35. Stepien, C. A. & Brusca, R. C. Nocturnal attacks on nearshore fishes in southern California
601 by crustacean zooplankton. *Marine Ecology Progress Series* **25**, 91–105 (1985).
602 36. Warner, J. A. & Case, J. F. The zoogeography and dietary induction of bioluminescence in
603 the midshipman fish, *Porichthys notatus*. *The Biological Bulletin* **159**, 231–246 (1980).
604 37. Cohen, A. C. & Oakley, T. H. Collecting and processing marine ostracods. *J. Crustacean*
605 *Biol.* **37**, 347–352 (2017).
606 38. Lee, K. H.-H. Genetic differentiation in *Vargula tsujii* (Ostracoda: Cypridinidae) along the
607 California coast. (California State University, Los Angeles, 2002).
608 39. Paradis, E. pegas: an R package for population genetics with an integrated-modular
609 approach. *Bioinformatics* **26**, 419–420 (2010).
610 40. R Core Team. R: A Language and Environment for Statistical Computing. (2017).
611 41. Jombart, T. adegenet: a R package for the multivariate analysis of genetic markers.
612 *Bioinformatics* **24**, 1403–1405 (2008).
613 42. Schwarz, G. Estimating the Dimension of a Model. *Ann. Stat.* **6**, 461–464 (1978).
614 43. Vannier, J., Abe, K. & Ikuta, K. Feeding in myodocopid ostracods: functional morphology
615 and laboratory observations from videos. *Mar. Biol.* **132**, 391–408 (1998).
616 44. Schindelin, J. *et al.* Fiji: an open-source platform for biological-image analysis. *Nat. Methods*
617 **9**, 676–682 (2012).
618 45. Pedregosa, F. *et al.* Scikit-learn: Machine Learning in Python. *J. Mach. Learn. Res.* **12**,
619 2825–2830 (2011).
620 46. Van Rossum, G. & Drake, F. L., Jr. *Python tutorial*. (Centrum voor Wiskunde en Informatica
621 Amsterdam, 1995).
622 47. Weisenfeld, N. I., Kumar, V., Shah, P., Church, D. M. & Jaffe, D. B. Direct determination of
623 diploid genome sequences. *Genome Res.* **27**, 757–767 (2017).
624 48. Ogoh, K. & Ohmiya, Y. Complete mitochondrial DNA sequence of the sea-firefly, *Vargula*
625 *hilgendorfii* (Crustacea, Ostracoda) with duplicate control regions. *Gene* **327**, 131–139

626 (2004).
627 49. Langmead, B. & Salzberg, S. L. Fast gapped-read alignment with Bowtie 2. *Nat. Methods* **9**,
628 357–359 (2012).
629 50. Nurk, S. *et al.* Assembling Genomes and Mini-metagenomes from Highly Chimeric Reads. in
630 *Lecture Notes in Computer Science* 158–170 (2013).
631 51. Wick, R. R., Schultz, M. B., Zobel, J. & Holt, K. E. Bandage: interactive visualization of de
632 novo genome assemblies. *Bioinformatics* **31**, 3350–3352 (2015).
633 52. Camacho, C. *et al.* BLAST+: architecture and applications. *BMC Bioinformatics* **10**, 421
634 (2009).
635 53. Priyam, A. *et al.* Sequenceserver: a modern graphical user interface for custom BLAST
636 databases. *bioRxiv* 033142 (2015). doi:10.1101/033142
637 54. Robinson, J. T. *et al.* Integrative genomics viewer. *Nat. Biotechnol.* **29**, 24–26 (2011).
638 55. Shen, W., Le, S., Li, Y. & Hu, F. SeqKit: A Cross-Platform and Ultrafast Toolkit for FASTA/Q
639 File Manipulation. *PLoS One* **11**, e0163962 (2016).
640 56. Walker, B. J. *et al.* Pilon: an integrated tool for comprehensive microbial variant detection
641 and genome assembly improvement. *PLoS One* **9**, e112963 (2014).
642 57. Bernt, M. *et al.* MITOS: improved de novo metazoan mitochondrial genome annotation. *Mol.*
643 *Phylogenet. Evol.* **69**, 313–319 (2013).
644 58. Jeffery, N. W., Ellis, E. A., Oakley, T. H. & Gregory, T. R. The genome sizes of ostracod
645 crustaceans correlate with body size and evolutionary history, but not environment. *J.*
646 *Hered.* **108**, 701–706 (2017).
647 59. Cohen, A. C. & Morin, J. G. Patterns of reproduction in ostracodes: a review. *Journal of*
648 *Crustacean Biology* **10**, 184 (1990).
649 60. Wakayama, N. Embryonic development clarifies polyphyly in ostracod crustaceans. *Journal*
650 *of Zoology* **273**, 406–413 (2007).
651 61. Lewis, S. M. & Cratsley, C. K. Flash signal evolution, mate choice, and predation in fireflies.

652 *Annu. Rev. Entomol.* **53**, 293–321 (2008).
653 62. Deheyn, D. D. Bioluminescence in the brittle star *Amphipholis squamata* (echinodermata):
654 an overview of 10 years of research. in *Bioluminescence and Chemiluminescence* (2001).
655 doi:10.1142/9789812811158_0009
656 63. Houliston, E., Momose, T. & Manuel, M. *Clytia hemisphaerica*: a jellyfish cousin joins the
657 laboratory. *Trends Genet.* **26**, 159–167 (2010).
658 64. Boissin, E., Hoareau, T. B., Féral, J. P. & Chenuil, A. Extreme selfing rates in the
659 cosmopolitan brittle star species complex *Amphipholis squamata*: data from progeny-array
660 and heterozygote deficiency. *Mar. Ecol. Prog. Ser.* **361**, 151–159 (2008).
661 65. Heip, C. The life-cycle of *Cyprideis torosa* (Crustacea, Ostracoda). *Oecologia* **24**, 229–245
662 (1976).
663 66. Martens, K. Effects of temperature and salinity on postembryonic growth in *Mytilocypris*
664 *henricae* (Chapman) (Crustacea, Ostracoda). *Journal of Crustacean Biology* **5**, 258–272
665 (1985).
666 67. Viviani, V. R. Fireflies (Coleoptera: Lampyridae) from southeastern Brazil: habitats, life
667 history, and bioluminescence. *Ann. Entomol. Soc. Am.* **94**, 129–145 (2001).
668 68. Ho, J.-Z., Chiang, P.-H., Wu, C.-H. & Yang, P.-S. Life cycle of the aquatic firefly *Luciola ficta*
669 (Coleoptera: Lampyridae). *J. Asia. Pac. Entomol.* **13**, 189–196 (2010).
670 69. Fu, X., Nobuyoshi, O., Vencl, F. V. & Lei, C. Life cycle and behaviour of the aquatic firefly
671 *Luciola leii* (Coleoptera: Lampyridae) from Mainland China. *Can. Entomol.* **138**, 860–870
672 (2006).
673 70. Soong, K., Lin, Y., Chao, S. & Chang, D. Spawning time of two shallow-water brittle stars.
674 *Mar. Ecol. Prog. Ser.* **376**, 165–171 (2009).
675 71. Hagman, D. K. & Vize, P. D. Mass spawning by two brittle star species, *Ophioderma*
676 *rubicundum* and *O. Squamosissimum* (Echinodermata: Ophiuroidea), at the Flower Garden
677 Banks, Gulf of Mexico. *Bull. Mar. Sci.* **72**, 871–876 (2003).

678 72. Rivers, T. J. & Morin, J. G. Female ostracods respond to and intercept artificial conspecific
679 male luminescent courtship displays. *Behav. Ecol.* **24**, 877–887 (2013).
680 73. Stern, D. L. & Orgogozo, V. Is Genetic Evolution Predictable? *Science* **323**, 746–751 (2009).
681 74. Boake, C. R. B. *et al.* Genetic Tools for Studying Adaptation and the Evolution of Behavior.
682 *The American Naturalist* **160**, S143 (2002).
683 75. Ritchie, M. G. Sexual Selection and Speciation. *Annu. Rev. Ecol. Evol. Syst.* **38**, 79–102
684 (2007).
685 76. Yeh, H.-W. & Ai, H.-W. Development and applications of bioluminescent and
686 chemiluminescent reporters and biosensors. *Annu. Rev. Anal. Chem.* (2019).
687 doi:10.1146/annurev-anchem-061318-115027
688 77. Cong, L. *et al.* Multiplex genome engineering using CRISPR/Cas systems. *Science* **339**,
689 819–823 (2013).
690 78. Krzywinski, M. *et al.* Circos: an information aesthetic for comparative genomics. *Genome*
691 *Res.* **19**, 1639–1645 (2009).
692 79. Pang, K. & Martindale, M. Q. Mnemiopsis leidyi Spawning and Embryo Collection. *CSH*
693 *Protoc.* **2008**, db.prot5085 (2008).
694 80. Warren, K. J. The establishment and characterization of primary cell cultures derived from
695 the ctenophore *Mnemiopsis leidyi*. (University of Miami, 2016).
696 81. Baker, L. D. & Reeve, M. R. Laboratory culture of the lobate ctenophore *Mnemiopsis*
697 *mccradyi* with notes on feeding and fecundity. *Marine Biology* **26**, 57–62 (1974).
698 82. Kahn, B. Scientists Have Cultivated a Mesmerizing Jelly That's Like 'Barely Organized
699 Water'. *Earther* (2018). Available at: https://earther.gizmodo.com/scientists-have-cultivated-
700 a-mesmerizing-jelly-thats-li-1823207295. (Accessed: 28th June 2019)
701 83. Lindner, A. & Migotto, A. E. The life cycle of *Clytia linearis* and *Clytia noliformis*: metagenic
702 campanulariids (Cnidaria: Hydrozoa) with contrasting polyp and medusa stages. *Journal of*
703 *the Marine Biological Association of the United Kingdom* **82**, 541–553 (2002).

84. Delroisse, J., Ortega-Martinez, O., Dupont, S., Mallefet, J. & Flammang, P. De novo transcriptome of the European brittle star *Amphiura filiformis* pluteus larvae. *Mar. Genomics* **23**, 109–121 (2015).

85. Oba, Y. *et al.* Bioluminescence of a firefly pupa: involvement of a luciferase isotype in the dim glow of pupae and eggs in the Japanese firefly, *Luciola lateralis*. *Photochem. Photobiol. Sci.* **12**, 854–863 (2013).

86. Watkins, O. C., Sharpe, M. L., Perry, N. B. & Krause, K. L. New Zealand glowworm (*Arachnocampa luminosa*) bioluminescence is produced by a firefly-like luciferase but an entirely new luciferin. *Sci. Rep.* **8**, 3278 (2018).

87. Meyer-Rochow, V. B. Glowworms: a review of *Arachnocampa* spp. and kin. *Luminescence* **22**, 251–265 (2007).

88. Takaie, H. Ten years of the glow-worm (*Arachnocampa richardsae*) rearing at Tama Zoo--Fascination of a living milky way. *Insectarium* **34**, 336–342 (1997).

89. Maheswarudu, G. & Vineetha, A. Culture of the littoral oligochaete *Pontodrilus bermudensis* Beddard. *The Journal of Bioprocess Technology* **97**, 142–155 (2013).

90. Nishida, H. Development of the appendicularian *Oikopleura dioica*: culture, genome, and cell lineages. *Dev. Growth Differ.* **50 Suppl 1**, S239–56 (2008).

91. Martí-Solans, J. *et al. Oikopleura* dioica culturing made easy: a low-cost facility for an emerging animal model in EvoDevo. *Genesis* **53**, 183–193 (2015).

Figures

Figure 1. Map of localities where collections (and attempted collections of *Vargula tsujii* were made). Black points represent geographic annotations for reference, purple points refer to the location where ostracods were collected that were ultimately cultured, blue where animals were found or collected, orange where Kornicker originally collected animals, and red where no *V. tsujii* were found. (A) Map of the California (USA) coastline where *V. tsujii* collections were attempted; (B) Map of the region near Two Harbors (Santa Catalina Island, California, USA) where *V. tsujii* collections were attempted.

Figure 2. Diagrammatic representation of aquarium setup for sea fireflies. (A) Source water flows into (B) a reservoir tank, which overflows to keep the reservoir full and water level constant. (C) We use a siphon to carry water from a reservoir tank to main aquarium where ostracods live. Water level of the main tank drains through sand (stippled), through (E) an outflow that is raised to a level that would cause water to remain at the level of the dashed line, even if a siphon is interrupted to cause water to stop flowing into the main tank. (F) Plastic bottle and parts used to create small aquarium using the same logic as main aquarium. (G) Custom-built acrylic aquarium with drain in bottom and raised outflow with adjustable rate.

Figure 3. Figure 3. Haplotype networks for (A) COI sequences, and (B) 16S sequences of *Vargula tsujii* animals from three localities sampled. Abbreviations: CI, Catalina Island; SD, San Diego; SP, San Pedro.

Figure 4. Embryogenesis within brooding females of *V. tsujii* post release into the marsupium. (A) Day 0, (B) Day 1-4, (C) Day 5-7, (D) Day 8-9, (E) Day 10-13, (F) Day 14-17, (G) Day 18-19, (H) Day 20-21, (I) Day 22-23, (J) Day 25-38.

755 **Figure 5.** Summary of the timing of embryogenesis stages in *V. tsujii*. This represents the
756 complete range of first appearance of each features across multiple broods, including: yolk
757 separation (range = 5-8 days, N = 7); eye spot formation (range = 10-18 days, N = 12); upper lip
758 formation (range = 15-19 days, N = 3); limb formation (range = 18-23 days, N = 11); hatching
759 (range = 25-38 days, N = 11).
760
761 **Figure 6.** (A) K-means clusters of *Vargula tsujii* developmental stages based on carapace
762 height and width. Instar stages were assigned to each cluster via comparison to *P.*
763 *annecohenae* and additional analysis of male and female size dimorphism. (B) Points
764 representing laboratory cultured animals overlayed on wild caught and unknown data. Different
765 colors represent different clusters in the k-means analysis, and are labeled with their inferred
766 instar/adult stages. (C) Shows wild-caught animals dissected and identified as female in relation
767 to the k-means clusters, and (D) shows wild-caught animals dissected and identified as male in
768 relation to the k-means clusters.
769
770 **Figure 7.** Mitochondrial genome of V. tsujii. Note the duplicated control regions, CR1 and CR2
771 (in gray). Figure produced with Circos [78].
772
773
774
775
776
777
778
779
780

781 **Tables**

782 **Table 1.** Species of bioluminescent metazoans for which cultures are known to exist, including
783 information on the luciferin used for luminescence, estimated generation times, and whether the
784 luciferin used is synthesized via the genome of the luminescent organism itself (autogenic).

Species	**Phylum**	**Luciferin**	**Autogenic luciferin?**	**Generation time**	**Citations**
Mnemiopsis leidyi, Bolinopsis infundibulum, Leucothea pulchra	Ctenophora	coelenterazine	Possibly	~13 days (based on *M. mccradyi*)	[80–83]
Clytia haemispherica	Cnidaria	coelenterazine	No	~14 days (based on other *Clytia*)	[65,84]
Amphiura filiformis	Echinodermata	coelenterazine	No	Unknown	[85]
Photuris spp. Aspisoma lineatum Aquatica lateralis Aquatica ficta	Arthropoda	beetle luciferin	Yes	3-24 months	[17,69,70,86]
Arachnocampa richardsae	Arthropoda	glow worm luciferin	Possibly	10-12 months	[87–89]
Pontodrilus litoralis	Annelida	earthworm luciferin	?	1-3 months	[90]
Oikopleura dioica	Chordata	?	?	5 days	[91,92]

785

786

787

788 **Table 2.** List of collections locations or attempted collection locations for *Vargula tsujii*.

789 Collection locations for which a latitude and longitude could not be determined were not figured,

790 but are included here.

Number	Location	Latitude	Longitude	Collected?
1	WMSC, Santa Catalina Island, CA, USA	33.445139	-118.4845	Yes
2	Shelter Island boat launch, San Diego, CA, USA	32.69	-117.223028	Yes
3	Cabrillo Beach, San Pedro, CA, USA	33.713306	-118.283673	Yes
4	Goleta Beach Pier, Goleta, CA, USA	34.414065	-119.828707	Yes
5	Santa Catalina Island, CA, USA	33.375	-118.6105556	Yes [33]
6	Un-named site	33.3805556	-117.5819444	Yes [33]
7	Un-named site	33.5797222	-118.1380556	Yes [33]
8	Santa Monica Pier, Santa Monica, CA, USA	34.0008333	-118.5777778	Yes [33]
9	Pinos Point, Pacific Grove, CA, USA	36.6658333	-121.9583333	Yes [33]
10	Seaport Village Pier, San Diego, CA, USA	32.708943	-117.171855	No

11	Shelter Island Police Dock, San Diego, CA, USA	32.709057	-117.235108	No
12	Mission Point, San Diego, CA, USA	32.761427	-117.245091	No
13	Mission Bay - Pacific Passage, San Diego, CA, USA	32.773906	-117.210387	No
14	Dana Point Harbor, Dana Point, CA, USA	33.460975	-117.699136	No
15	Balboa Peninsula Point, Newport Beach, CA, USA	33.599048	-117.884112	No
16	Balboa Beach Pier, Newport Beach, CA, USA	33.6075	-117.9288	No
17	Los Alamitos Bay, Long Beach, CA, USA	33.752434	-118.113842	No
18	Redondo Beach, CA, USA	33.84519	-118.395764	No
19	Marina del Rey, CA, USA	33.976286	-118.445642	No
20	Santa Monica Pier, Santa Monica, CA, USA	34.0093	-118.4967	No
21	Prisoners Harbor, Channel Islands National Park, CA, USA	34.020384	-119.684361	No
22	Ventura Harbor boat ramp, Ventura, CA, USA	34.249224	-119.263238	No

23	Ventura Harbor Pier, Ventura, CA, USA	34.273498	-119.291992	No
24	Santa Barbara Harbor, Santa Barbara, CA, USA	34.406417	-119.690501	No
25	Santa Barbara Harbor boat ramp, Santa Barbara, CA, USA	34.408094	-119.692132	No
26	Stearns Wharf, Santa Barbara, CA, USA	34.411296	-119.687706	No
27	Monterey Bay Pier, Monterey, CA, USA	36.6050389	-121.8919972	No
28	Monterey Bay Aquarium, Monterey CA, USA	36.6186583	-1219014222	No
29	Half Moon Bay, CA, USA	37.501913	-122.482173	No
30	Bodega Harbor, Bodega Bay, CA, USA	38.3333806	-123.0497833	No
-	La Jolla, CA, USA	unknown	unknown	Yes [33]
-	Bahia Los Angeles, Baja California, Mexico	unknown	unknown	Yes [33]

Table 3. Measurements for each cluster (and inferred instar) of *Vargula tsujii* ± SD.

Instar	**N**	**Carapace Length (mm) ± SD**	**Carapace Height (mm) ± SD**	**Eye width (mm) ± SD**
Embryo	84	0.418 +- 0.0271	0.326 + 0.0112	0.0630 + 0.0112
A-V	106	0.687 +- 0.0504	0.427 ± 0.0289	0.0682 + 0.0164
A-IV	89	0.863 +- 0.0448	0.517 ± 0.0374	0.0684 + 0.0271
A-III	66	1.078 +- 0.0516	0.632 ± 0.0494	0.121 + 0.0208
A-II	96	1.214 +- 0.0426	0.711 ± 0.0409	0.133 + 0.0160
Male A-1/Female A-1/ Adult Male	106	1.581 +- 0.0605	0.913 ± 0.0402	0.226 + 0.0345
Adult Female?	70	1.983 +- 0.0798	1.154 ± 0.0591	0.210 + 0.0326

810 **Table 4**: Comparison of embryogenesis timing between five different ostracod species post-

811 deposition. Species with an asterisk (*) are bioluminescent cypridinids.

Species	Cloudy Embryo	Yolk Sep.	Eye Spot Formation	Upper Lip	Limbs	Release	Citation
*Vargula annecohenae**	2-3 days	9 days	14-15 days	17 days	-	19 days	[27]
Euphilomedes carcharodonta	-	14 days	58-70 days	-	14-41 days	65-75 days	[30]
*Vargula hilgendorfii**	-	1-2 Days	6-8 days	6-8 days	4-5 days	16 days	[28]
*Vargula tsujii**	3-4 days	5-8 days	10-18 days	15-19 days	18-23 days	25-38 days	This study
Xestoleberis hanaii	-	-	-	-	-	9-11 days	[32]

812

813

814

815

816

817

818

819

820

821

822

823

824

825

826

827 **Supplementary Materials**

828 **Table S1.** List of specimens examined in this paper for which sequences were obtained,
829 including locality, museum collection numbers (where applicable), and GenBank accession
830 numbers for the two genes sequenced (COI and 16S).

831

832 **Table S2.** Raw measurements of *Vargula tsujii* individuals, including carapace height and
833 length, keel width and eye width.

834

835 **Table S3.** Unfiltered library sequencing statistics for *V. tsujii*.

836

837 **Figure S1.** Traversal of the cleaned SPAdes *V. tsujii* mitochondrial genome assembly graph
838 nodes plotted by Bandage (gray). The single circularizing path representing the collapsed
839 duplicate control regions are shown in blue. The black stroke shows the path traversed through
840 the assembly graph followed to produce the circularized mtDNA FASTA file with two control
841 region, matching the structure of the V. hilgendorfii mtDNA (Ogoh and Ohmiya 2004).

842

843 **Figure S2.** Results for our 16S DAPC model test to determine the number of clusters that is
844 favored via comparison of Bayesian Information Criterion (BIC) values.

845

846 **Figure S3.** Results for our COI DAPC model test to determine the number of clusters that is
847 favored via comparison of Bayesian Information Criterion (BIC) values.

848

849 **Figure S4.** Cluster membership based on our 16S DAPC analysis compared with the original
850 population designation for each specimen. Overall, the clusters are not representative of any
851 population-level structure.

852

853 **Figure S5.** Cluster membership based on our 16S DAPC analysis compared with the original
854 population designation for each specimen. Overall, the clusters are not representative of any
855 population-level structure.
856
857 **Figure S6.** Exploded diagram of custom aquarium for rearing *Vargula tsujii*. A photo of built
858 aquarium is in main text, Figure 2. **A**. Plumbing components include 1. PVC pipe 1.5 inch
859 diameter. 2. PVC socket ball valve to control the rate of outflow 3. PVC 1.5 inch elbows 4. PVC
860 elbow with one side threaded to screw into 5. threaded bulkhead to span bottom of aquarium for
861 drainage 6. float switch valve to control water level (not shown on Figure 2 of main text). **B**.
862 Acrylic panels of ¼ inch thickness welded together with solvent include 7. Two panels of
863 dimension 16.5 x 13.25 inches that form the long sides of the aquarium 8. Two panels of
864 dimension 8 x 10.75 inches that form the short sides of the aquarium. One of these panels has
865 a hole drilled for the water inflow and float switch 9. One panel of 16.5 x 7.5 inches to form the
866 bottom of the aquarium, including a hole drilled for the bulkhead 10. One panel of 16.5 x 7.5
867 inches to forms a false bottom for the aquarium similar to the bottom of an undergravel
868 aquarium filter. We drilled small holes throughout to allow water but not sand to flow through.
869 (Not shown on Figure 2). In practice, we welded legs on the false bottom to allow it to stand on
870 the true bottom of the aquarium above the height of the bulkhead drain.